

To be submitted to ApJ

ENERGETIC CORRELATION BETWEEN SOLAR FLARES AND CORONAL MASS EJECTIONS

Brian R. Dennis¹, Drew A. Medlin², Leah Hagg^{3,4}, Richard A. Schwartz^{1,5}, and
A. Kimberley Tolbert^{1,5}

*Solar Physics Branch, Code 612.1,
NASA Goddard Space Flight Center, Greenbelt, MD 20771*

ABSTRACT

We find a strong correlation between the kinetic energies (KEs) of the coronal mass ejections (CMEs) and the radiated energies of the associated solar flares for the events that occurred during the period of intense solar activity between 18 October and 08 November 2003. CME start times, speeds, mass and KEs were taken from Gopalswamy et al. (2005), who used SOHO/LASCO observations. The GOES observations of the associated flares were analyzed to find the peak soft X-ray (SXR) flux, the radiated energy in SXRs (L_{SXR}), and the radiated energy from the emitting plasma across all wavelengths (L_{hot}). RHESSI observations were also used to find the energy in non-thermal electrons, ions, and the plasma thermal energy for some events. For two events, SORCE/TIM observations of the total solar irradiance during a flare were also available to give the total radiated flare energy (L_{total}). We find that the total flare energies of the larger events are of the same order of magnitude as the CME KE with a stronger correlation than has been found in the past for other time intervals. The following rule-of-thumb (good to an order of magnitude for the larger events) can be used to relate flare and CME energies: $L_{total} \simeq 10 L_{hot} \simeq 100 L_{SXR} \simeq \text{CME KE}$.

Subject headings: Sun: flares, Sun: Coronal Mass Ejections (CMEs), Sun: X-rays

¹NASA Goddard Space Flight Center

²NRAO

³The Catholic University of America

⁴Johns Hopkins University

⁵SSAI

1. Introduction

Since Gosling exposed the solar flare myth (Gosling 1993), we have known that coronal mass ejections are the most geoeffective of the various transient solar phenomena. It is now known that solar energetic particles (SEPs) are accelerated primarily in the CME shock. The magnetic storms and induced currents on the Earth result from the impact of the CME magnetic fields on the magnetosphere. Solar flares, in contrast, are now thought to be largely confined to the vicinity of the Sun. The electrons and ions accelerated in a flare generally lose their energy in the lower corona and chromosphere with only the electromagnetic radiation escaping. Thus, their effects on the Earth are primarily caused by the impact of this radiation on the upper atmosphere and the interference effects of the radio emission.

The association between flares and CMEs has been evident since the first detection of CMEs. A CME, particularly the faster variety ($> 1000 \text{ km s}^{-1}$), is usually accompanied by a flare, although there are examples where this does not appear to be the case. Sometimes when an accompanying flare is not observed, the source of the CME may be over the limb, but there are other cases where this does not seem to be the explanation. The great extent over the solar disc of CMEs compared to flares and the apparent early start of some CMEs before the flare impulsive phase also bring into question any causal relationship between them. There are many flares, especially smaller ones, where no CMEs are observed at all. Sometimes an eruption is observed with a flare but it doesn't continue to propagate and develop into a CME (Saint-Hilaire & Benz 2003).

Previous studies of flares and CMEs have shown a large scatter in correlations of various properties, bringing into question the physical relation between the two phenomena (Hundhausen 1999). In this paper, we report on the correlation between all flares and CMEs that occurred during the three-week interval in 2003 between October 18 and November 8, when there was an unprecedented number of large events. We chose this period since most of the events clearly came from one of three active regions as they transited the visible solar disc, so there is little ambiguity in most cases about where the events originated. There was almost full coverage of the X-ray flares with GOES and of the CMEs with LASCO on SOHO. Furthermore, two of the largest flares were also detected as an increase in the total solar irradiance by the Total Irradiance Monitor (TIM) on the SORCE mission (Woods et al. 2004). RHESSI observed at least parts of many of the flares in X-rays and detected gamma rays in two of them. Thus, there is a comprehensive and consistent set of both flare and the CME observations that can be used to determine various parameters, including estimates of the total energies involved in each case.

An energetics analysis of the X17 event on 28 October 2003 has already been published by Emslie et al. (2005) using all available observations. They show that the total energy

released during the flare is comparable (within an order of magnitude of 10^{32} ergs) to the total energy of the CME. The flare energy is made up of the energy of the accelerated electrons and ions and the energy of the hot plasma; the CME energy is principally in the kinetic energy of the erupting material. The SORCE measurements of the increase in total solar irradiance during the X17 flare on October 28 gives us possibly the most accurate measurement ever obtained for the total energy released during a flare. The irradiance increase integrated over the duration of the flare gives a total radiated energy from the flare (L_{total}) of 5×10^{32} ergs (Kopp et al. 2004; Woods & Kopp 2005). Surprisingly, the irradiance peaked during the impulsive phase of the flare, i.e., on the rise of the soft X-ray flux seen with GOES. Again in this case, the CME kinetic energy was comparable at 1.2×10^{33} ergs. Unfortunately, RHESSI did not observe the impulsive phase of this flare so no detailed breakdown of the flare energy can be made. Nevertheless, the total radiated energy in soft X-rays (L_{SXR}) can be readily determined from the GOES observations. Also, as described by Emslie et al. (2005), the total energy radiated at all wavelengths from the hot, SXR-emitting plasma (L_{hot}) can be estimated from the plasma temperature and emission measure derived from the two-channel GOES data using the method given by White et al. (2005) based on the CHIANTI atomic data base and radiation code (Dere et al. 1997; Landi et al. 2006). L_{SXR} gives a hard lower limit on the total energy of the flare with only the assumption that the observed soft X-rays are emitted isotropically from the flare site. L_{hot} is also a lower limit on the flare energy subject only to the assumption of isotropic emission from a thermal plasma all at the same temperature, and with coronal abundances as defined in CHIANTI (v. 5.1). For this flare, $L_{SXR} = 3 \times 10^{30}$ ergs and $L_{hot} = 3 \times 10^{31}$ ergs, i.e., a factor of ~ 100 and ~ 10 smaller than the SORCE value for L_{total} , respectively. Presumably, the additional radiated energy seen by TIM but not measured with GOES must be at longer wavelengths, i.e. $> 10 \text{ \AA}$.

In this paper, we present the results of a similar comparison between the kinetic energies of all CMEs observed with LASCO in this three-week period and the radiated energies (L_{SXR} and L_{hot}) determined from the GOES soft X-ray observations of the corresponding flares. We also include estimates of the energies in flare-accelerated electrons and ions obtained from RHESSI X-ray and gamma-ray observations when available for these and other well observed flares.

2. Observations and Data Analysis

Included in this analysis are all 80 CMEs observed with LASCO (Gopalswamy et al. 2005) and the 151 flares above the GOES C1 class reported for the period from 18 Oct. to 8 Nov. 2003. There were 11 X, 21 M, and 26 C-class flares. The flare on 4 November 2003

saturated the GOES detectors but has been estimated to be one of the top three X-ray events ever recorded, peaking at the X30.6 level (Kiplinger & Garcia 2004). Only 58 of the CMEs had an apparently associated flare that occurred within ± 50 minutes of the estimated CME initiation time. Energy estimates have been made for all of these CMEs and the associated flares, and a detailed correlation analysis carried out. Additional flare and CME energy estimates for the X1.5 flare on 21 April, 2002, and the X4.8 flare on 23 July, 2002, taken from Emslie et al. (2004, 2005) were also used in this study. Energetics parameters of all the CMEs and associated flares used in the subsequent analysis for this paper are listed in Table 1.

2.1. CME Energies

The kinetic energies of the CMEs were obtained from Gopalswamy et al. (2005). They estimated the plane-of-sky velocities from the height-to-time plots determined from the CME positions in the LASCO C2 and C3 fields taken every 12 minutes. The estimated velocities range from ~ 62 to $2,700 \text{ km s}^{-1}$. The total mass of the moving material was estimated from the luminosity seen in the same LASCO images. The uncertainties in the kinetic energy determined in this way are typically a factor of two, providing the CME appears in at least three LASCO images so that an accurate estimate can be made of the velocity. The increase in gravitational potential energy was also estimated but found to be negligible compared to the kinetic energy in all but the slowest CME, which had a velocity of only 62 km s^{-1} .

The CME start times were generally taken from the SOHO/LASCO CME CATALOG (http://cdaw.gsfc.nasa.gov/CME_list/), where linear fits to the height-to-time plots were extrapolated back to the time when the CME would have been at one solar radius. This technique works well for CMEs showing a constant velocity. However, some CMEs show evidence for acceleration or, in some cases, deceleration in the LASCO C2 and/or C3 height-to-time plots. In these cases, linear fits to all LASCO height-to-time data clearly yield incorrect start times. For these CMEs, only the first few data points from the height-to-time data are used for a linear fit and this was extrapolated back to 1 solar radius to obtain a more likely start time.

2.2. Flare Energies

For each flare, values of L_{SXR} and L_{hot} were obtained as follows. First, plots of the GOES two-channel light curves were obtained using the GOES Workbench now available in

SSW by typing “GOES” at the IDL command line. Data with 3-s time resolution were used as available from the Solar Data Analysis Center (SDAC) at Goddard Space Flight Center. All gain-change spikes were removed and a background subtracted (usually equal to the flux just preceding the initial rise in the 1 – 8 Å channel). L_{SXR} was then obtained by summing the remaining Watts m^{-2} over the duration of the flare, i.e., $L_{SXR} = \sum (F_i \delta t)$ where F_i is the measured flux in interval i , δt is 3 s, and i covers all intervals during the flare. The flare end time for this purpose was defined as the time when the flux returned to the pre-flare background level or when it started to rise again at the start of a subsequent flare.

The values of L_{SXR} obtained in this way are subject to systematic uncertainties dependent on the plasma temperature. This is because constant conversion factors are used to relate the measured current in the GOES soft X-ray detectors to the incident flux in Watts m^{-2} (White et al. 2005). The temperature dependence of these factors is explicitly included in the calculation of L_{hot} when the temperature (T) and emission measure (EM) are obtained from the background-subtracted fluxes in the two channels using the prescription given by (White et al. 2005). We used the CHIANTI atomic data base (version 5.1) and coronal abundances for these calculations. The values calculated for L_{hot} in this way assume a single-temperature plasma. This gives a lower limit to the total radiated energy from the hot plasma because the radiant energy flux is near a minimum at the typical temperatures of 10 - 20 MK obtained from these calculations. Thus, if there is plasma at lower temperatures, it would add to the estimate made by assuming that all of the plasma were at the higher temperature.

Various functions are available of the total radiant energy over all wavelengths from a hot plasma as a function of temperature. We choose, for convenience, to use the relation provided in CHIANTI (v. 5.1) since it is in general agreement with other published curves (Aschwanden 2004). Thus, we calculate the radiant energy flux R_i for each 3-s interval and sum the product over the duration of the flare as for the calculation of L_{SXR} , i.e., $L_{hot} = \sum (R_i \delta t)$. Note that for this calculation, it is not necessary to know the volume of the plasma. This is a major advantage over the method for estimating the plasma thermal energy U_{th} from EM, T, and the volume determined from RHESSI X-ray images. In that case, uncertainties arise because of the unknown third dimension of the source along the line of sight and the volume filling factor, the fraction of the observed volume actually filled with the hot plasma. In this case, $U_{th} = 3 N_e k T$ ergs, where N_e is the total number of electrons in the plasma, and k is Boltzman’s constant. Since $N_e = n_e V$, where n_e is the electron density, and $EM = n_e^2 V$, we have that $U_{th} = 3 k T \sqrt{EM V_{obs} f}$ where V_{obs} is the volume estimated from the RHESSI images and f is the filling factor relating V_{obs} to V , the actual volume of the radiating plasma. The volume can be estimated from the 2-dimensional line-of-sight images obtained with RHESSI with assumptions about the source extent along

the line of sight and the filling factor. RHESSI images give the area (A_{obs}) of the source and we use the relation $V_{obs} = A_{obs}^{3/2}$ to get an estimate of the area. The filling factor is usually taken to be one to give an upper limit on the total plasma energy but it has variously been estimated to be as low as 10^{-4} under certain circumstances. A detailed comparison between L_{hot} and U_{th} is beyond the scope of this paper.

3. Results

Of the 80 CMEs detected with LASCO, seven were determined to have originated on the backside of the Sun by comparing the extrapolated CME start time with EIT movies of that time interval. Only 58 of the 151 C1 or greater flares could be reasonably connected to a specific CME. Thus, 79% of the frontside CMEs (58 of 73) were associated with a flare, and 38% of the flares (58 of 151) were associated with a CME. See Table 1 for a complete list of all CMEs and flares used in the subsequent analysis.

There is a tendency for the CMEs to start after the associated flares. This is shown in fig. 1, where the histogram of CME delays after the flare start times is plotted in 10 minute intervals. The mean CME delay is 8.3 min. but this could be explained by the sometimes large uncertainties in the extrapolated CME start times and by the acceleration prior to the appearance of the CME in the LASCO C2 field.

Values of L_{SXR} and L_{hot} are plotted against the kinetic energy of the associated CME in figures 2 and 3, respectively. Out of the 58 flares with associated CMEs, only 51 had enough signal above the pre-flare background to give meaningful T and EM values from the GOES Workbench. Both L_{SXR} and L_{hot} show the following power-law relations when compared to the CME KE:

$$\text{CME KE} = 83 L_{SXR}^{0.95}$$

$$\text{CME KE} = 10 L_{hot}^{0.89}$$

Fig. 3 also shows the energies given in Table 2 for other events where the CME KE and different components of the energy of the associated flare have been reported in the literature. The values of L_{total} are plotted for the two flares that show a definitive increase in the total solar irradiance as measured with TIM on the SORCE mission. The energies in the accelerated electrons and ions derived from the RHESSI hard X-ray and gamma-ray measurements, respectively, are shown for three events as reported by Emslie et al. (2005) and Share (private communication).

Fig. 4 shows a linear correlation between the CME kinetic energy and the GOES peak

flux for the associated flare of the form $\text{CME KE}/10^{30} = 0.2 \times \text{GOES Peak flux}$. In addition to all of the flares plotted in Figs. 2 and 3, this plot also includes the seven flares that were too weak to allow values of L_{SXR} and L_{hot} to be calculated. Fig. 5 shows that there is also a positive correlation between the CME speed and the GOES peak flux of the form $\text{CME speed} = 390 \times (\text{GOES peak flux})^{0.22}$.

The correlations between the peak GOES SXR flux, L_{SXR} , L_{hot} , and the CME KE are all better than previous studies have shown. A Kendall's tau nonparametric correlation (`r_correlate.pro`, IDL v. 6.2) was used to test for correlations. L_{SXR} and L_{hot} show correlation coefficients of 0.65 and 0.67, respectively. Note that there is no significantly better correlation found by choosing to compare either L_{SXR} or L_{hot} to the CME KE. The correlation coefficients relating the peak SXR flux to the CME KE and speed are 0.61 and 0.42, respectively in good agreement with previous findings (Yashiro et al. 2002; Burkepile et al. 2004).

4. Discussion

The CME KEs and the radiated energies of associated flares for the period from 18 October through 08 November, 2003, are more strongly correlated than previous studies of events over longer time intervals have shown (Yeh et al. 2005). The radiated energy in SXR (L_{SXR}) is approximately two orders of magnitude lower than the CME KE while the total radiated energy from the hot SXR-emitting plasma at all wavelengths is approximately one order of magnitude lower than the CME KE. The *SORCE/TIM* measurements for the two flares observed by *TIM* indicate that the total radiated energy (L_{total}) for those two events is of the same order of magnitude as the CME KE. Thus, the following rule of thumb can be used to estimate the total energy radiated by a flare from the other estimated energies:

$$L_{total} \simeq \text{CME KE} \simeq 10L_{hot} \simeq 100L_{SXR}$$

If all flares could be observed by *TIM*, and they all had a measured radiated energy about an order of magnitude higher than measured by *GOES*, then most flares would have radiated energies of the same order of magnitude as CMEs generated from that active region. Why the flares and CMEs from this time period have a tighter relationship between the CME KE and radiated energy of the associated flare is not apparent. Previous studies show weaker correlations, but also include a much broader time span for analysis.

5. Acknowledgments

CHIANTI is a collaborative project involving the NRL (USA), RAL (UK), MSSL (UK), the Universities of Florence (Italy) and Cambridge (UK), and George Mason University (USA).

The CME catalog is generated and maintained at the CDAW Data Center by NASA and The Catholic University of America in cooperation with the Naval Research Laboratory. SOHO is a project of international cooperation between ESA and NASA.

REFERENCES

- Aschwanden, M. J. 2004, *Physics of the Solar Corona. An Introduction* (Praxis Publishing Ltd., Chichester, UK)
- Burkepile, J. T., Hundhausen, A. J., Stanger, A. L., St. Cyr, O. C., & Seiden, J. A. 2004, *Journal of Geophysical Research (Space Physics)*, 109, 3103
- Dere, K. P., Landi, E., Mason, H. E., Monsignori Fossi, B. C., & Young, P. R. 1997, *A&AS*, 125, 149
- Emslie, A. G., Dennis, B. R., Holman, G. D., & Hudson, H. S. 2005, *Journal of Geophysical Research (Space Physics)*, 110, 11103
- Emslie, A. G., Kucharek, H., Dennis, B. R., Gopalswamy, N., Holman, G. D., Share, G. H., Vourlidas, A., Forbes, T. G., Gallagher, P. T., Mason, G. M., Metcalf, T. R., Mewaldt, R. A., Murphy, R. J., Schwartz, R. A., & Zurbuchen, T. H. 2004, *Journal of Geophysical Research (Space Physics)*, 109, 10104
- Gopalswamy, N., Yashiro, S., Liu, Y., Michalek, G., Vourlidas, A., Kaiser, M. L., & Howard, R. A. 2005, *Journal of Geophysical Research (Space Physics)*, 110, 9
- Gosling, J. T. 1993, *J. Geophys. Res.*, 98, 18937
- Hundhausen, A. 1999, in *The many faces of the sun: a summary of the results from NASA's Solar Maximum Mission.*, ed. K. T. Strong, J. L. R. Saba, B. M. Haisch, & J. T. Schmelz, 143
- Kiplinger, A. L. & Garcia, H. A. 2004, *American Astronomical Society Meeting Abstracts*, 36, 739

- Kopp, G., Lawrence, G. M., Rottman, G., & Woods, T. 2004, *Bulletin of the American Astronomical Society*, 36, 669
- Landi, E., Del Zanna, G., Young, P. R., Dere, K. P., Mason, H. E., & Landini, M. 2006, *ApJS*, 162, 261
- Saint-Hilaire, P. & Benz, A. O. 2003, *Sol. Phys.*, 216, 205
- White, S. M., Thomas, R. J., & Schwartz, R. A. 2005, *Sol. Phys.*, 227, 231
- Woods, T. N., Eparvier, F. G., Fontenla, J., Harder, J., Kopp, G., McClintock, W. E., Rottman, G., Smiley, B., & Snow, M. 2004, *Geophys. Res. Lett.*, 31, 10802
- Woods, T. N. & Kopp, G. 2005, *AGU Fall Meeting Abstracts*, A7+
- Yashiro, S., Gopalswamy, N., Michalek, G., & Howard, R. A. 2002, *Bulletin of the American Astronomical Society*, 34, 695
- Yeh, C.-T., Ding, M. D., & Chen, P. F. 2005, *Sol. Phys.*, 229, 313

Table 1. CME and Flare Properties

C2 Date	Image UT	R_{Sun} UT	Vel. km/s	Mass gms	KE erg	GOES UT	Start Class	L_{hot} erg	L_{SXR} erg	Delay min.
2002										
04/21	01:27	...	2393	...	2.0E+32	00:40	X1.5	1.9E+31		
07/23	00:42	00:27	2285	...	1.0E+32	00:15	X4.8	9.3E+30	1.5E+30	12
2003										
10/18	05:54	05:15	707	1.1E+14	2.8E+29	05:31	C2.0	1.6E+26	9.8E+26	-16
10/18	09:07	08:39	778	1.8E+14	5.6E+29	08:47	C3.3	7.0E+28	3.3E+27	8
10/18	20:59	20:25	652	2.5E+15	5.3E+30	20:18	C3.3	1.4E+29	8.0E+27	7
10/18	23:55	22:38	544	5.9E+15	8.8E+30	22:14	C6.7	5.6E+28	3.9E+27	24
10/19	06:54	06:22	798	2.7E+14	8.7E+29	06:08	M1.9	4.7E+29	4.0E+28	14
10/19	08:30	07:35	469	8.6E+14	9.5E+29	07:21	C1.7	14
10/19	17:08	16:30	472	7.2E+15	8.1E+30	16:29	X1.1	1.8E+30	2.4E+29	1
10/19	19:52	18:50	799	1.3E+15	4.2E+30	19:21	M1.0	1.0E+29	6.5E+27	-16
10/19	22:30	22:05	469	3.2E+14	3.5E+29	22:00	C1.9	5
10/21	03:54	03:45	1484	1.2E+16	1.3E+32
10/21	16:06	15:35	533	7.7E+14	1.1E+30	15:08	C2.3	4.8E+28	5.5E+27	27
10/21	19:54	19:08	720	5.9E+15	1.5E+31	19:22	M2.4	8.0E+30	4.9E+29	-14
10/21	20:58	19:15	602	6.6E+15	1.0E+31
10/21	23:30	23:15	824	8.3E+14	2.8E+30	22:58	M2.4	1.1E+30	1.6E+29	17
10/22	01:31	00:25	666	3.8E+15	8.3E+30
10/22	03:54	03:28	1163	5.8E+15	2.9E+31	03:28	M3.7	5.1E+30	2.9E+29	0
10/22	08:30	07:20	719	1.1E+16	2.8E+31
10/22	15:30	15:10	1054	2.7E+14	1.5E+30	15:06	M1.4	1.1E+29	6.0E+27	4
10/22	16:30	15:56	1040	2.7E+14	1.5E+30	15:57	M1.2	9.8E+28	5.6E+27	-1
10/22	20:06	19:54	1085	9.7E+15	5.7E+31	19:47	M9.9	2.3E+30	2.8E+29	7
10/23	03:06	02:33	656	6.4E+14	1.4E+31	02:35	M2.4	1.2E+29	1.5E+28	-2
10/23	07:31	07:10	1090	1.1E+14	6.4E+29	07:02	M3.2	1.5E+29	1.2E+28	8
10/23	08:54	08:25	1406	1.2E+16	1.2E+32	08:19	X5.4	6.1E+30	1.1E+30	6
10/23	13:54	13:11	511	8.1E+14	1.1E+30	12:58	C5.1	8.4E+28	1.5E+28	13
10/23	20:06	19:52	1136	1.1E+16	7.2E+31	19:50	X1.1	1.6E+30	1.7E+29	2
10/24	02:54	02:39	1055	1.2E+16	6.9E+31	02:27	M7.6	2.6E+30	2.7E+29	7
10/24	05:30	05:15	1233	1.0E+15	7.9E+30	05:04	M4.2	4.1E+29	3.0E+28	11
10/24	16:30	15:27	384	2.1E+15	1.5E+30	15:23	C8.9	2.4E+30	1.3E+29	4
10/24	20:06	19:28	399	1.0E+15	8.2E+29	18:42	M1.3	4.2E+29	2.2E+28	46
10/25	05:18	04:27	685	4.4E+15	1.0E+31	04:17	M1.2	1.5E+30	6.3E+28	10
10/25	08:30	07:21	235	1.4E+14	3.8E+28	07:10	C4.7	11
10/26	01:31	00:42	419	2.8E+15	2.4E+30	00:43	C3.2	1.2E+29	3.1E+27	-1
10/26	05:30	04:08	684	7.2E+15	1.7E+31
10/26	06:54	06:25	1371	1.2E+16	1.2E+32	6:07	X1.2	7.5E+30	9.1E+29	28
10/26	08:30	00:03	258	1.4E+16	4.6E+30
10/26	10:34	10:12	929	1.0E+14	4.4E+29	10:06	C1.1	6
10/26	17:54	17:32	1537	2.0E+16	2.4E+32	17:21	X1.2	1.3E+31	1.1E+30	11
10/27	04:30	03:37	481	2.4E+15	2.8E+30	03:34	C8.6	4.9E+28	2.1E+28	5
10/27	05:06	04:20	323	2.0E+14	1.1E+29	04:12	M1.2	1.2E+30	4.8E+28	8
10/27	08:30	08:04	1322	4.5E+15	2.9E+31	07:51	M2.7	5.4E+30	2.0E+29	13
10/27	13:31	12:25	1005	4.1E+14	2.1E+30	12:27	M6.7	9.4E+29	1.1E+29	-2

Table 1—Continued

C2 Date	Image UT	R_{Sun} UT	Vel. km/s	Mass gms	KE erg	GOES UT	Start Class	L_{hot} erg	L_{SXR} erg	Delay min.
10/27	20:30	19:46	990	9.5E+14	4.7E+30	19:48	C9.0	4.2E+29	1.8E+28	-2
10/28	05:54	04:55	602	4.9E+13	8.9E+28	05:07	C7.7	1.0E+29	3.9E+27	-12
10/28	06:30	06:00	684	1.6E+14	3.8E+29	05:54	C5.0	5.2E+28	3.3E+27	6
10/28	07:31	06:23	394	6.7E+13	5.2E+28	05:54	C5.7	1.4E+29	1.3E+28	6
10/28	09:30	09:08	853	1.5E+15	5.5E+30	09:06	C6.0	2.1E+28	7.4E+27	2
10/28	10:54	10:34	1054	1.1E+15	6.1E+30	10:18	M8.1	6.3E+29	2.3E+29	16
10/28	11:30	11:06	2459	4.0E+16	1.2E+33	10:58	X17	2.1E+31	3.4E+30	8
10/29	10:16	08:10	922	1.6E+17	7.0E+32
10/29	20:54	20:45	2029	1.6E+16	3.4E+32	20:37	X10	8.8E+30	1.7E+30	8
10/31	04:42	04:23	2126	7.1E+14	1.6E+31	04:26	M2.0	1.7E+29	1.5E+28	-3
10/31	07:02	09:30	62	7.5E+14	1.4E+28	21:20	C3.6	1.0E+28	3.9E+27	10
10/31	17:30	16:27	309	8.8E+14	4.2E+29	16:18	C2.1	4.7E+27	1.1E+27	-2
10/31	20:30	19:40	605	6.7E+13	1.2E+29	19:21	C3.3	19
11/01	12:30	11:00	246	1.6E+15	4.7E+29
11/01	14:54	13:35	334	7.5E+15	4.2E+30	13:26	C4.2	9
11/01	21:30	20:00	413	4.9E+15	4.2E+30	19:44	C2.8	16
11/01	23:06	22:35	899	8.9E+15	3.6E+31	22:26	M3.2	6.4E+29	4.6E+28	9
11/02	09:30	9:10	2036	4.5E+16	9.3E+32
11/02	11:30	10:50	826
11/02	17:30	17:19	2598	4.9E+15	1.6E+32	17:03	X8.3	9.9E+30	1.8E+30	16
11/03	01:59	1:32	827	6.6E+15	2.3E+31	01:09	X2.7	4.4E+30	7.0E+29	23
11/03	10:06	9:53	1420	1.3E+16	1.3E+32	9:43	X3.9	6.5E+30	1.1E+30	10
11/03	19:31	18:40	641	2.0E+14	4.2E+29	18:26	C3.5	1.4E+29	2.2E+27	14
11/04	12:06	11:55	1208	1.1E+16	8.3E+31
11/04	12:54	10:20	605	2.3E+15	4.2E+30	10:11	M3	5.3E+29	4.7E+28	9
11/04	19:31	18:35	327	3.5E+15	1.8E+30	18:02	C7.7	2.4E+29	3.9E+28	33
11/04	19:54	19:40	2657	1.7E+16	6.1E+32	19:29	X30.6	2.6E+31	4.0E+30	11
11/05	16:54	16:22	1075	3.0E+14	1.7E+30	16:28	C1.9	9.0E+28	8.9E+27	6

Table 2: Reported energies (in units of 10^{30} ergs) of other well-observed CMEs and their associated flares.

Energy Component	21Apr02	23Jul02	28Oct03	3Nov03	4Nov03
CME					
Kinetic Energy	200	100	1200	130	610
Gravitational potential	5	13
Flare					
GOES Class	X1.5	X4.8	X17	X3.9	X31
L_{hot}	19	9	42	11	44
Electrons > 20 keV	20	30	...	190	...
Ions > 1 MeV	<40	79	80	30	...
Thermal Plasma, $T > 5$ MK	0.08	0.08	0.16	0.036	0.41

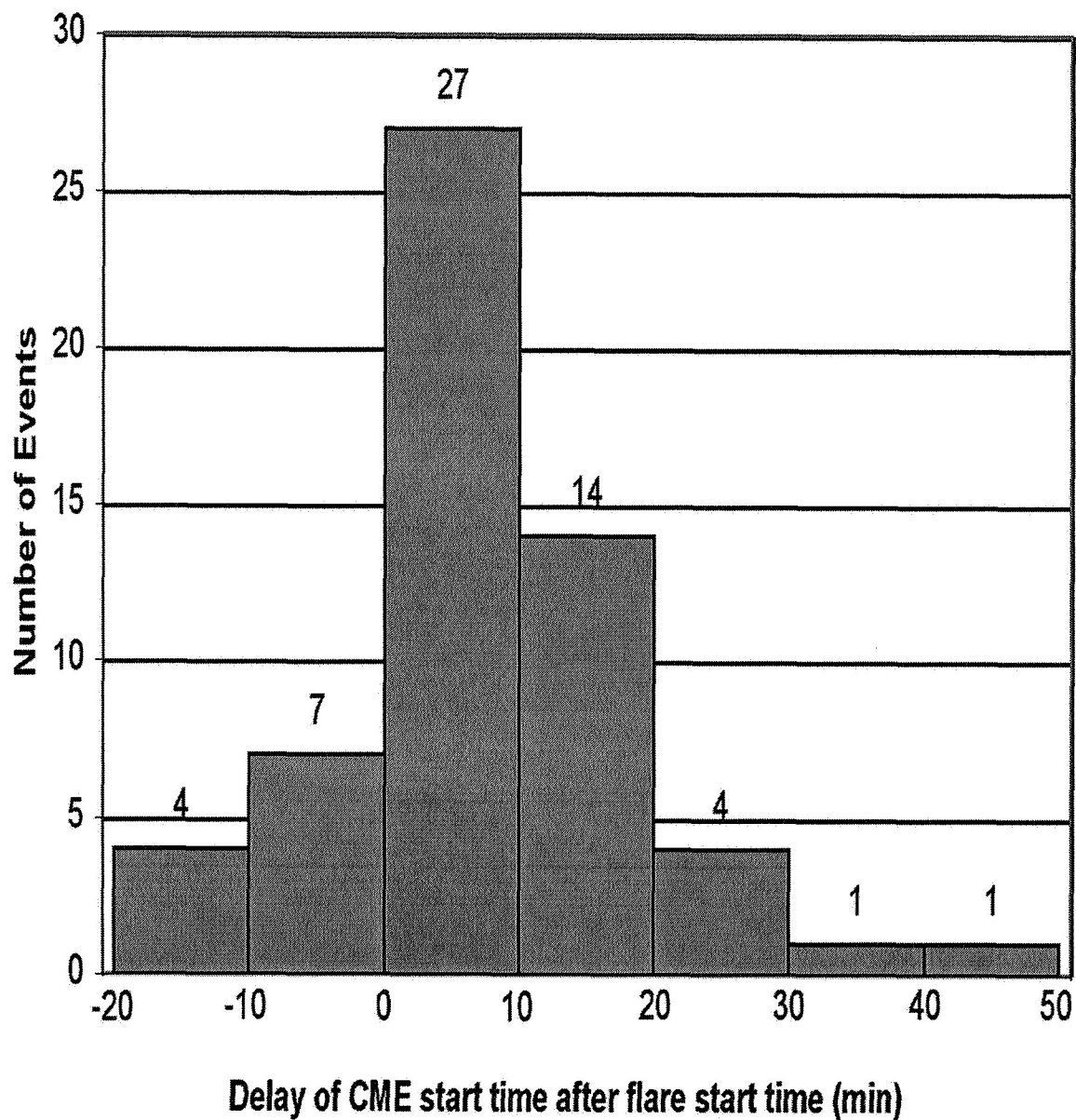


Fig. 1.— Histogram of the CME delays after the start of the associated flares. The CME start time was estimated by extrapolating the LASCO height-to-time curves back to the solar surface. The flare start times were determined from the GOES 1 – 8 Å light curves. The largest number of CMEs (27 out of 58, ~ 46%) start between 0 and 10 minutes after the start of the associated GOES flare.

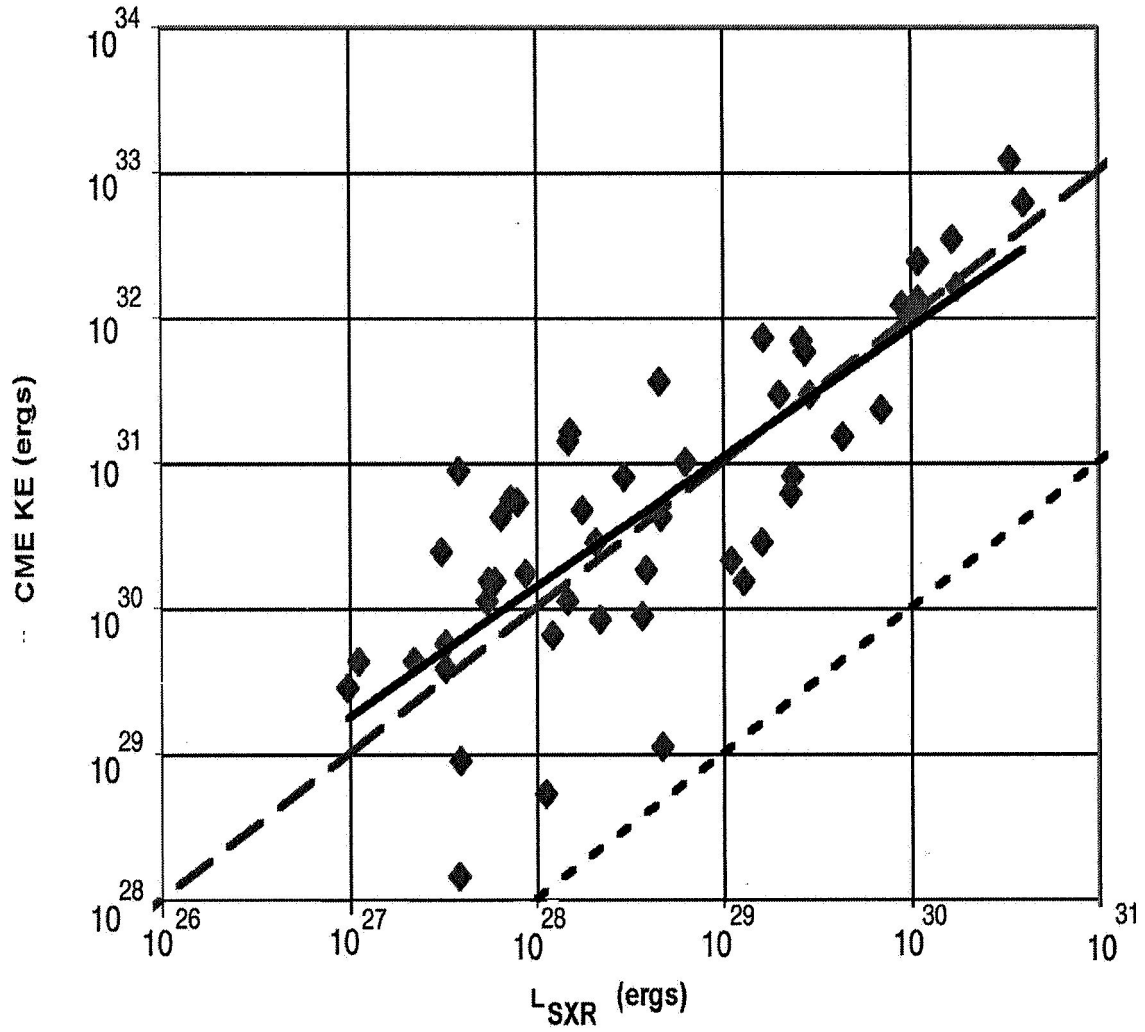


Fig. 2.— The CME kinetic energy vs. the energy radiated in soft X-rays by the associated flare. Solid line represents a power-law fit to the data points of the form $\text{CME KE} = 83 L_{SXR}^{0.9}$ ergs. Broken line is for $\text{CME KE} = 100 L_{SXR}$. Dotted line shows equality of the CME and flare energies.

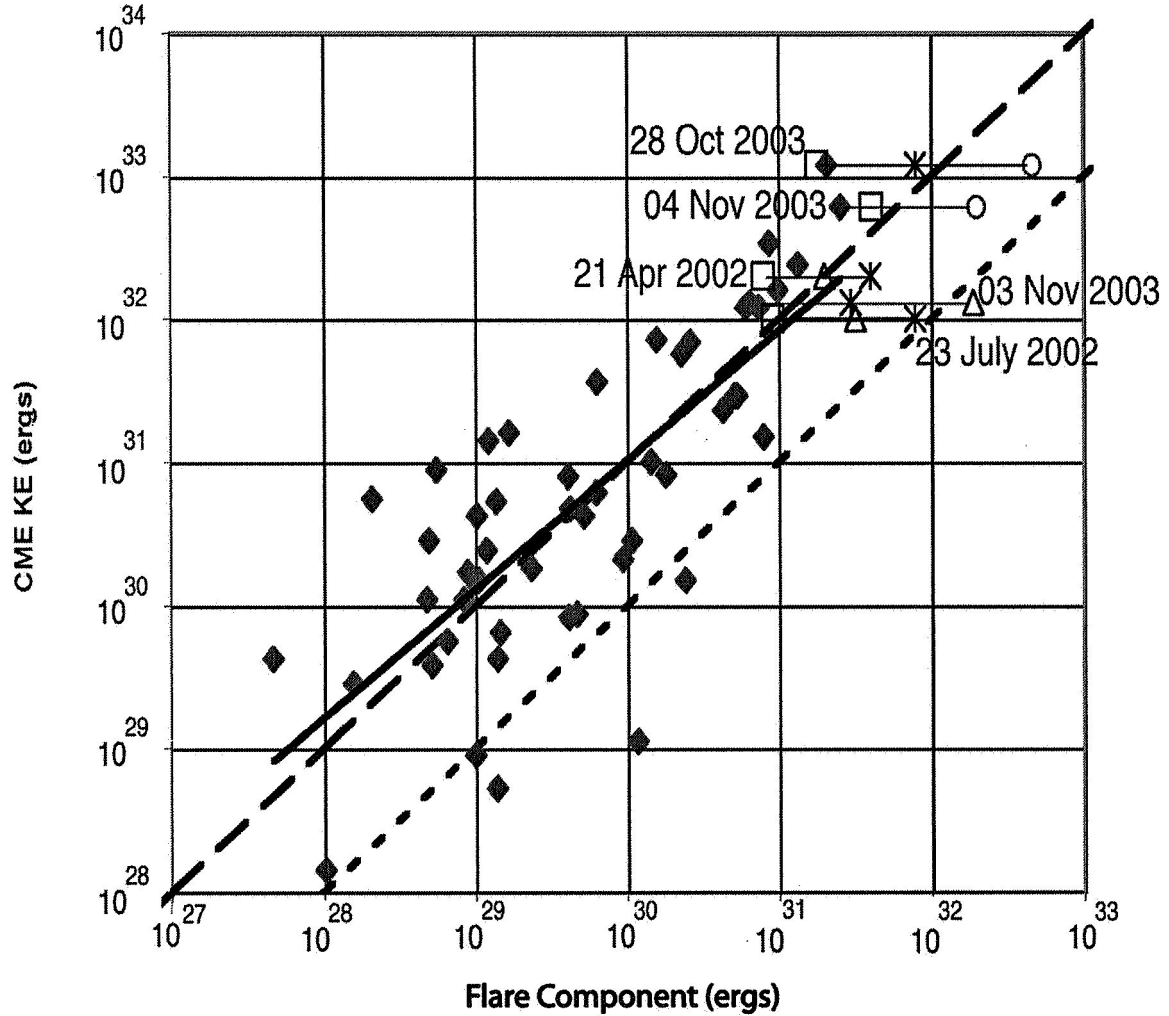


Fig. 3.— The CME kinetic energies vs. various components of the energies of the associated flares. Filled diamonds - L_{hot} , the total radiated energy from the SXR-emitting plasma of the associated flares; stars - the energy in ions > 1 MeV estimated from the gamma rays; triangles - energy in electrons > 20 keV estimated from the hard X-ray spectrum; open squares - the peak thermal energy of the plasma seen in SXRs; open circles - the SORCE/TIM measurements of the increase in the total solar irradiance during the two flares indicated; solid line - a power-law fit to the L_{hot} data points of the form $CME\ KE = 10 L_{hot}^{0.9}$ ergs; dotted line shows equality of the CME and flare energies; broken line is for CME KEs equal to ten times the flare energies.

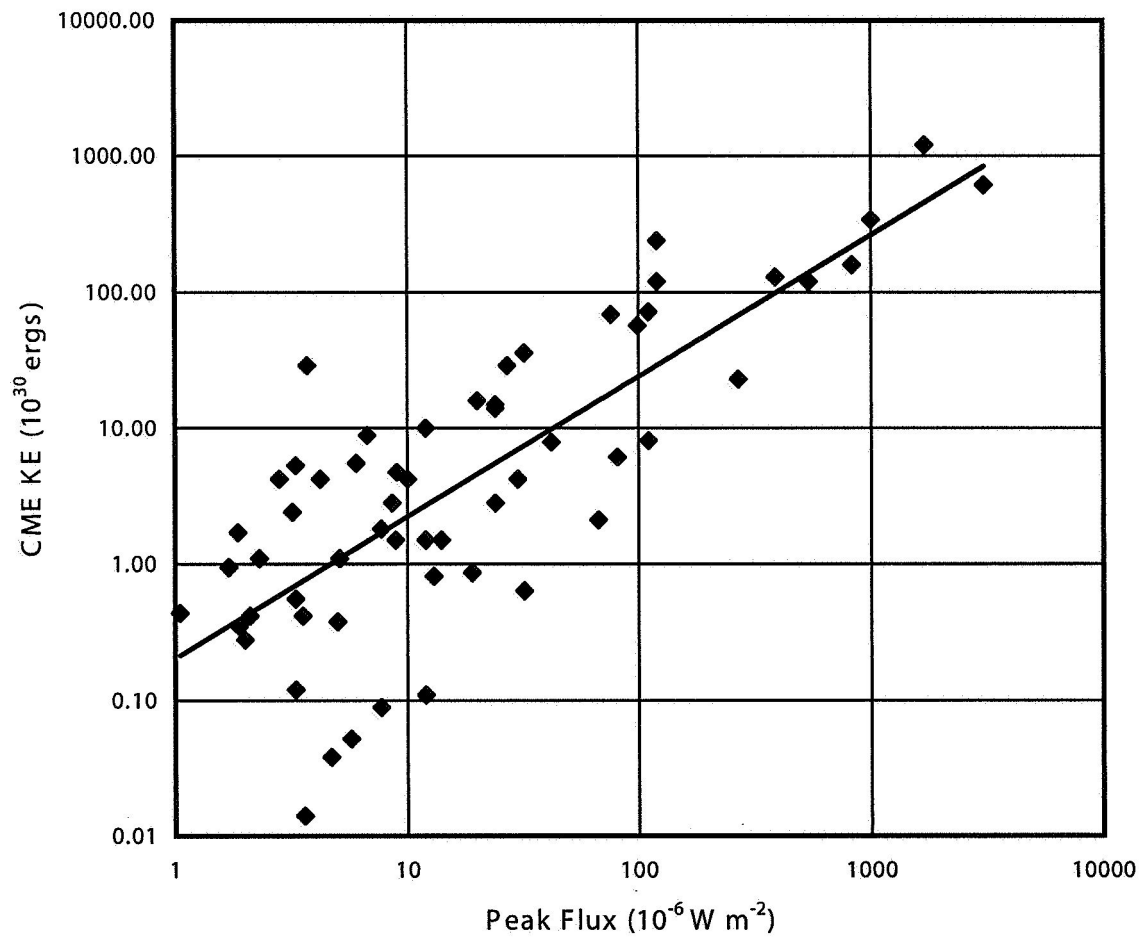


Fig. 4.— CME kinetic energy vs. peak GOES SXR flux.

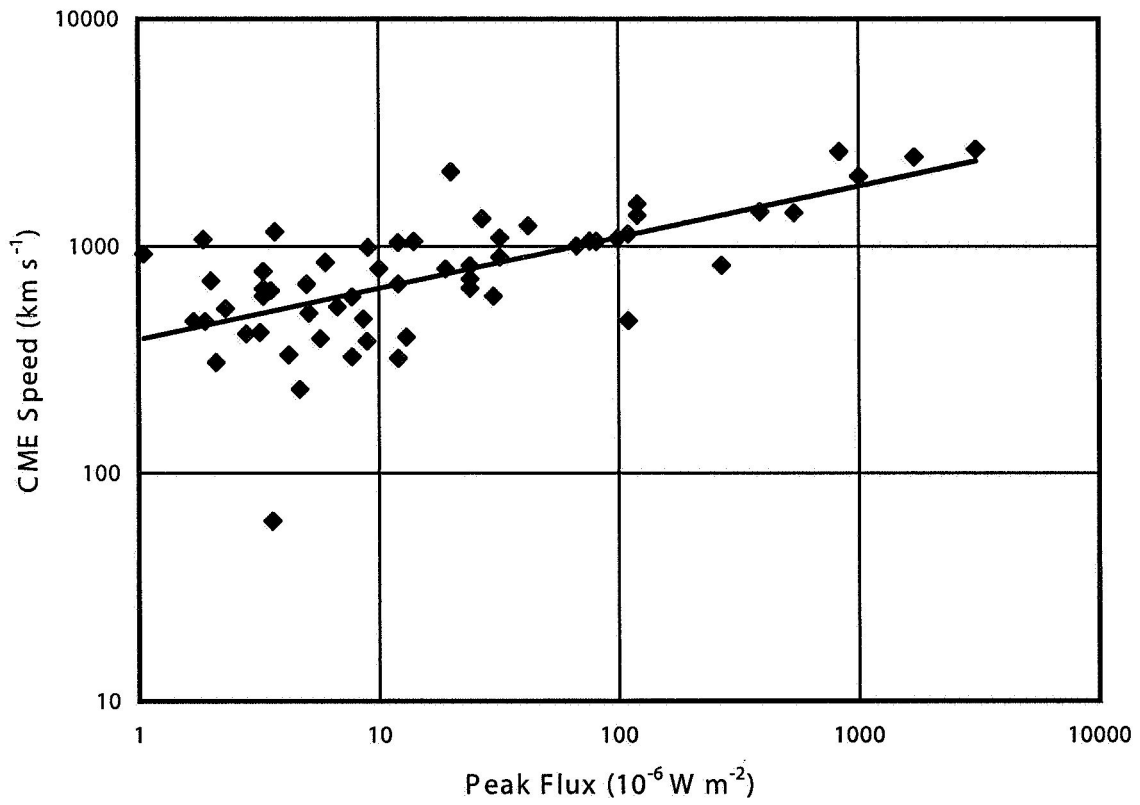


Fig. 5.— CME average speed vs. peak GOES SXR flux.

Brian R. Dennis

From: Brian R. Dennis [Brian.R.Dennis@nasa.gov]
Sent: Thursday, August 03, 2006 4:51 PM
To: 'Robert.J.Gutro.1@gsfc.nasa.gov'
Cc: Douglas M. Rabin (Douglas.M.Rabin@nasa.gov)
Subject: Popular Summary - ENERGETIC CORRELATION BETWEEN SOLAR FLARES AND CORONAL MASS EJECTIONS

Paper Title

ENERGETIC CORRELATION BETWEEN SOLAR FLARES AND CORONAL MASS EJECTIONS

Authors

Brian R. Dennis / Code 612.1
Drew A. Medlin / NRAO
Leah Haga / Johns Hopkins University
Richard A. Schwartz / SSAI
A. Kimberley Tolbert / SSAI

E-Mail Addresses

Brian R. Dennis (Brian.R.Dennis@nasa.gov)
Drew Medlin (dmedlin@nrao.edu)
Leah Haga (lbhaga@gmail.com)
Richard Alan Schwartz (Richard.A.Schwartz.1@gsfc.nasa.gov)
Anne Kimberley Tolbert (Anne.K.Tolbert.1@gsfc.nasa.gov)

Abstract:

We find a strong correlation between the kinetic energies (KEs) of the coronal mass ejections (CMEs) and the radiated energies of the associated solar flares for the events that occurred during the period of intense solar activity between 18 October and 08 November 2003. CME start times, speeds, mass and KEs were taken from Gopalswamy et al. (JGR, 110, A09S15, 2005), who used SOHO/LASCO observations. The GOES observations of the associated flares were analyzed to find the peak soft X-ray (SXR) flux, the radiated energy in SXR - L(SXR), and the radiated energy from the emitting plasma across all wavelengths L(hot). RHESSI observations were also used to find the energy in non-thermal electrons, ions, and the plasma thermal energy for some events. For two events, SORCE/TIM observations of the total solar irradiance during a flare were also available to give the total radiated flare energy - L(total). We find that the total flare energies of the larger events are of the same order of magnitude as the CME KE with a stronger correlation than has been found in the past for other time intervals. The following rule-of-thumb (good to an order of magnitude for the larger events) can be used to relate flare and CME kinetic energies (KEs) :

$$L(\text{total}) \sim 10 \times L(\text{hot}) \sim 100 \times L(\text{SXR}) \sim \text{CME KE.}$$

Popular Summary:

A solar flare is an explosion on the Sun that can be as energetic as ~1 billion 10 megaton hydrogen bombs going off in

8/7/2006

a few minutes. Coronal mass ejections are often associated with flares and involve the ejection of up to 100 million tons of material from the solar atmosphere out into space at speeds that can be over a million miles an hour. It is not known how these two phenomena are related but it has been thought that more energy was needed to accelerate the material of the CME than was released in the associated flare. In this paper, we compare different measures of the flare energy with estimates of the kinetic energy of associated CMEs for over 50 events recorded during the 3-week period of intense solar activity from 19 October to 4 November, 2003. We used the previously published CME kinetic energies from the SOHO coronagraph measurements and new estimates of the radiated energy from the associated flares from GOES X-ray observations. For one of the events, the Total Irradiance Monitor on the Solar Radiation and Climate Experiment (SORCE) had, for the first time, detected an increase in the total solar irradiance during a large flare, thus providing a firm lower limit on the total energy released by the flare. This turned out to be comparable to the kinetic energy of the associated CME and provided conversion factors to enable us to estimate the total energy released in a flare from other measures such as the total energy emitted in X-rays and the total energy radiated by the hot plasma produced by the flare. We find that the observations are consistent with the total energy released during a flare being ~10 times greater than the total energy radiated by the hot plasma over all wavelengths, ~100 times greater than the energy radiated in X-rays, but comparable to the kinetic energy of the associated CME. In retrospect, it may not be surprising that flare and CME energies are comparable. In the simplest model of these eruptive events, the energy is released in the corona by magnetic reconnection, with the material going up becoming the CME and the material going down making the flare. Equipartition of energy going up and going down might be expected in such a scenario. Of course, the situation is obviously much more complicated than such a simple-minded model would suggest. However, it is clear that the origins and energy sources of flares and CMEs are so intimately entwined that it is impossible to explain one without understanding the other. This is especially true now we know that flares are likely to be just as big energetically as CMEs. A popular science nugget on this subject can be found at the following web site:

http://sprg.ssl.berkeley.edu/%7Etohan/nuggets/?page=article&article_id=10